

Microstructural and Magneto-Optical Characterization of High J_c BSCCO-2223/Ag Tapes

J. Jiang*, T.C. Shields and J.S. Abell

School of Metallurgy and Materials, The University of Birmingham, Birmingham B15 2TT, UK

A. Polyanskii, D.M. Feldmann and D.C. Larbalestier

Applied Superconductivity Center, University of Wisconsin-Madison, WI 53706, USA

*Current address: Applied Superconductivity Center, University of Wisconsin-Madison, WI 53706, USA

Abstract — The phase and microstructural evolution, and critical current density of (Bi,Pb)-2223/Ag tapes prepared from a variety of precursor powders have been investigated. Correlations between the reaction kinetics, the microstructure and the critical current density are developed. A mechanism for the BSCCO-2223 phase formation depending on the precursor phase assemblage is presented. Magneto-optical imaging shows that high J_c samples ($J_c(77K, 0T) \sim 35 \text{ kA/cm}^2$) are well connected longitudinally but strongly sub-divided by longitudinal cracks. The performance of BSCCO-2223 tapes should be further improved by controlling the liquid phase to better heal the cracks.

I. INTRODUCTION

Superconducting Ag-sheathed (Bi,Pb)₂Sr₂Ca₂Cu₃O_x [Bi(Pb)-2223] tapes, produced by the oxide-powder-in-tube (OPIT) technique, have demonstrated the capacity to carry large currents at liquid nitrogen temperature for large scale engineering applications [1-3]. However, problems of reproducibility and developing high critical current densities while scaling up to practical lengths still remain. The basic reason seems to be that the processing of such complex materials at both nanometer and macroscopic scales is inherently complex. Cai et al. [4] recently used magneto-optical imaging to directly demonstrate that the transport J_c of very high J_c BSCCO-2223 tapes is more determined by their connectivity than by flux pinning and that an independent and much larger limiting influence on the J_c comes from unhealed cracks produced by deformation during the processing of the tapes.

Microstructural characterization of the Bi(Pb)-2223/Ag tapes is important for understanding the complex chemical phase relations in the Bi(Pb)-2223 system, and in particular the nature of the Bi-2223 phase and its texture development. Thurston et al. [5] first showed that synchrotron x-ray scattering techniques can effectively characterize many of the structural properties of the Bi-2223 superconducting tapes, because the high energy synchrotron radiation can penetrate through the whole tape. Here we have studied a number of tapes prepared under different circumstances by normal X-ray diffraction (XRD), scanning electron microscopy (SEM),

high energy synchrotron X-ray diffraction and magneto-optical (MO) imaging, in order to identify the dependence of microstructure and superconducting properties on processing variables.

II. EXPERIMENTAL

Powders were prepared by the solid state reaction method with different starting compositions and different calcination conditions. The silver-sheathed monofilamentary 2223 tapes were produced with the same processing parameters described previously [6]. The as-rolled tapes had a width of 2.2 mm and an overall thickness of 0.2 mm. The uniaxial pressure of 2 GPa was applied to all tapes at each intermediate pressing stage between sintering. The silver sheath was mechanically removed by cutting the tape sides for conventional X-ray diffraction (XRD). XRD peak intensities were determined by measuring the integrated area of the respective peaks.

Powder diffraction experiments were carried out at the UK SRS laboratory at Daresbury on station 9.1. According to the X-ray penetration depth measurement of Thurston et al. [5], a wavelength of 0.4868 Å, corresponding to X-ray energy of 25.47 keV, was chosen in our experiments. An image-plate based on a Molecular Dynamics Scanner was used for phase composition measurements. The image-plate is very useful when a diffraction peak is very weak; in particular, for identifying minor phases. The distance between sample and image plate was about 300 mm in all the experiments. The accurate distance was calibrated by using standard silicon powder diffraction. The beam size was 0.5x0.5 mm². The tape samples were attached horizontally to a holder using adhesive tape, and all patterns were recorded at room temperature. The beam was focused on the central area of the tape perpendicular to the tape surface.

TABLE I
NOMINAL COMPOSITION, THICKNESS AND J_c OF TAPES AFTER FINAL HEAT TREATMENT

Tape ID	Nominal Composition	Thickness(μm)	$J_c(\text{kA/cm}^2)$
SD	Bi _{1.8} Pb _{0.2} Sr ₂ Ca _{2.2} Cu ₃ O _x	~125	29
SG	Bi _{1.85} Pb _{0.35} Sr ₂ Ca _{2.2} Cu ₃ O _x	~125	32
MO1	Bi _{1.91} Pb _{0.29} Sr ₂ Ca _{2.2} Cu ₃ O _x	~125	27
MO2	Bi _{1.91} Pb _{0.29} Sr ₂ Ca _{2.2} Cu ₃ O _x	~105	33
MO3	Bi _{1.91} Pb _{0.29} Sr ₂ Ca _{2.3} Cu ₃ O _x	~105	34

Manuscript received Sept. 15 1998.

The work at Birmingham was supported by CLRC-UK and EPSRC and at UW by EPRI, AFOSR and benefited from facilities supported by the NSF supported MRSEC.

Samples for high energy X-ray diffraction and MO imaging are listed in Table 1. MO1 and MO3 were prepared for MO imaging by chemically removing the Ag cladding from a rolling plane face (the broad face of the tape) using a $\text{NH}_4\text{OH}/\text{H}_2\text{O}_2$ etch[7]. MO2 was examined without removing the Ag-cladding. MO imaging was performed by placing a ferromagnetic Bi-doped Y-iron-garnet film directly on the broad surface of the tape.

III. RESULTS AND DISCUSSION

A. Reaction kinetics of the Bi(Pb)-2223 phase and critical current density

Twenty three tapes fabricated from precursor powders with different nominal compositions and different calcination conditions were analyzed. The resultant phase assemblages of the calcined powders were different; the major phase was always 2212, with minor secondary phases consisting of Ca_2PbO_4 , CuO and Ca_2CuO_3 , the proportions of which depended on the particular combination of composition and calcination conditions. The optimum sintering temperature in air for these tapes to produce high J_c values was between 832 and 836°C[6]. The Bi-2223 formation in this temperature range was quite sluggish for some tapes, while for others it was quite fast. In order comprehensively to understand the reaction kinetics of the Bi-2223 phase, all the tapes were sintered at 836°C for 60 hours in air, regardless of precursor powder processing condition. This represents the first stage of the sintering/deformation cycles. The ratio of 2223 to 2212 and 2223 phases after the first sintering, as determined by XRD, was chosen as a criterion for the conversion or formation rate of the 2223 phase, since the same mechanical deformation parameters were used for all the tapes.

Fig.1 presents the critical current density of the fully processed tapes against the percent conversion from 2212 to 2223 of the corresponding tapes after the first sintering. It is

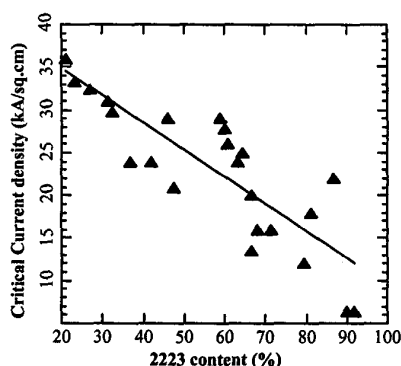


Fig. 1. Critical current density of the fully processed tapes against the percent conversion from 2212 to 2223 of the corresponding tapes after the first sintering in air at 836°C for 60 hours. The straight line is a guide to the eye.

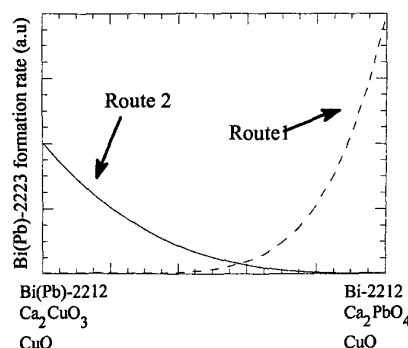


Fig. 2. Schematic description of the variation of the 2223 formation rate with the phase assemblage of the precursor powder for the two proposed reaction routes. Route 1: the liquid-assisted nucleation and growth process[12]; Route 2: the intercalation process[11].

clear that the precursor powders, which exhibited a slower formation rate of the 2223 phase correlate to a higher final J_c value. As discussed previously [8], one can control the formation rate of the 2223 phase by varying the nominal composition, phase assemblage and particle size of the precursor powder. However, studies by High et al. [9] have shown that non-superconducting phases grow more readily than the desired 2223 phase, due to lower activation energy for non-superconducting phase growth. One possible explanation why a slower formation rate of the 2223 phase corresponds to a higher final J_c value and a faster 2223 formation rate corresponds to a lower J_c is that the unreacted 2212 phase in the former case can react with the non-superconducting phases in the subsequent sinter stages, healing the cracks caused by the intermediate deformation between sintering. It can be seen in Fig. 1 that the data in the range of higher 2223 content are more scattered than those in the lower 2223 content range. J_c values are both higher and more reproducible from the precursor powders with a slower 2223 formation rate.

A combination of XRD and SEM examination established that the formation of the 2223 phase was always accompanied by the presence of Bi-2201 phase in tapes where the 2223 phase formed rapidly during the first cycle. It is believed that liquid is formed during the formation of the 2223 phase [10] and is facilitated by the Ca_2PbO_4 phase, which may be responsible for the faster formation of the 2223 phase in some tapes. We have suggested that extra liquid also leads to the rapid growth of alkaline earth cuprate, although the main role of the liquid phase is to promote the formation of the 2223 phase [6]. The formation of the 2201 phase was also associated with the formation of extra liquid phase during tape sintering. So we believe that 2201 precipitates from the liquid which forms during the transformation of the 2212 to 2223. This is consistent with the TEM work of Wang et al. [11], who observed the thin

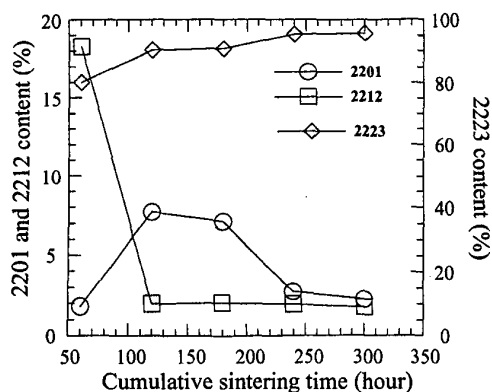


Fig. 3. Evolution of the 2201, 2212 and 2223 phases with sintering/deformation cycles for SD tapes

2201 layer between the 2212 and an amorphous region, which was considered to be liquid at the reaction temperature.

We have proposed that the formation of the Bi(Pb)-2223 phase is controlled by both the intercalation process and the liquid-assisted nucleation and growth, based on the effects of the precursor powder on the microstructure [8]. Fig. 2 sketches the proposed variation of the Bi(Pb)-2223 formation rate with the phase assemblage of the precursor for the two proposed processes. We further postulate that the maximum rate of the liquid-assisted process is higher than that of the intercalation. The combined formation rate is given by a combination of the two curves, from which it can be seen that there exists a minimum rate of 2223 formation when neither process is rapid.

Within this model, it can be explained why a slower 2223 formation rate corresponds to a higher J_c value and a faster formation rate corresponds to a lower J_c , as shown in Fig. 1. We believe that the phase assemblages in the tapes with slower formation rates are in the minimum rate region in Fig. 2. In this case, the formation of 2223 phase was controlled by both the two proposed routes. Although the formation rate is slower, it avoids the formation of the large amounts of the Bi-2201 and non-superconducting phases, while still maintaining enough liquid to heal the cracks caused by the intermediate deformation between sintering steps. So a higher J_c value can be achieved with such precursors. In the maximum 2223 growth rate region of the liquid-assisted route (route 1), we believe that rapid 2201 and non-superconducting phase growth is responsible for the lower J_c . In the maximum 2223 rate region of the intercalation route (route 2), lack of liquid phase is the reason for lower J_c , even though 2201 phase can be avoided by this route. According to Fig. 3, one can change the formation rate, in principle, of both routes from fast to slow and vice versa by controlling the precursor phase assemblage.

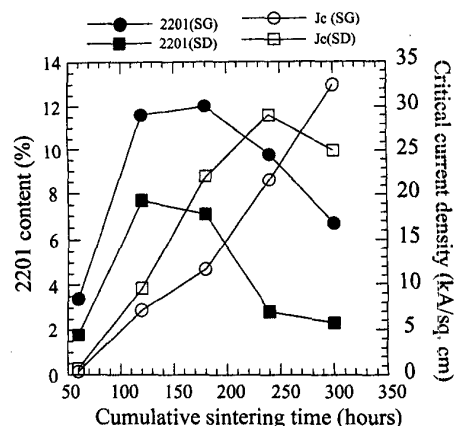


Fig. 4. Critical current density and 2201 phase evolution with sintering/deformation cycles for tapes SD and SG

B. High energy synchrotron X-ray diffraction

Fig. 3 quantitatively shows the evolution of the 2201, 2212 and 2223 phases with the sintering/deformation cycles for SD tapes. The relative amount of 2223 increased as the 2212 decreased, indicating that 2223 phase forms predominantly from the 2212 phase. However, the amount of the 2212 phase remained almost constant after the second sintering stage. The relative amount of the 2201 phase did not change monotonically, but first increased during the initial two stages and began to decrease after the third stage. A similar trend was also observed in the SG tapes shown in Fig. 4.

The critical current density evolution with the thermomechanical cycle is also shown in Fig. 4. Although the amount of the 2212 phase shown in Fig. 3 remained almost the same for tape SD after the second cycle, the J_c value was improved significantly during the third and fourth cycles. One possible reason is that the decrease of the amount of 2201 phase contributed to the improvement of J_c . This is also the reason why we need two more sintering/deformation cycles for a high J_c value even though the transformation of the 2212 to 2223 is nearly complete. Recently Wang et al. [13] have also shown that the J_c can be improved by removing the residual 2201 phase through a two-step sintering process. The measurements of Cai et al. [4] showed that there also exist some blocking c-axis current paths. Bi-2201 grains may play a significant role in blocking the current since they always lie parallel to the Bi-2223 grains and must be traversed when c-axis current flow is required to transmit from one grain to another.

C. Magneto-optical imaging

Fig. 5 shows the plan-view magneto-optical images of three tapes. A dominant feature of the MO images is that many light regions run in the longitudinal direction of the tape.

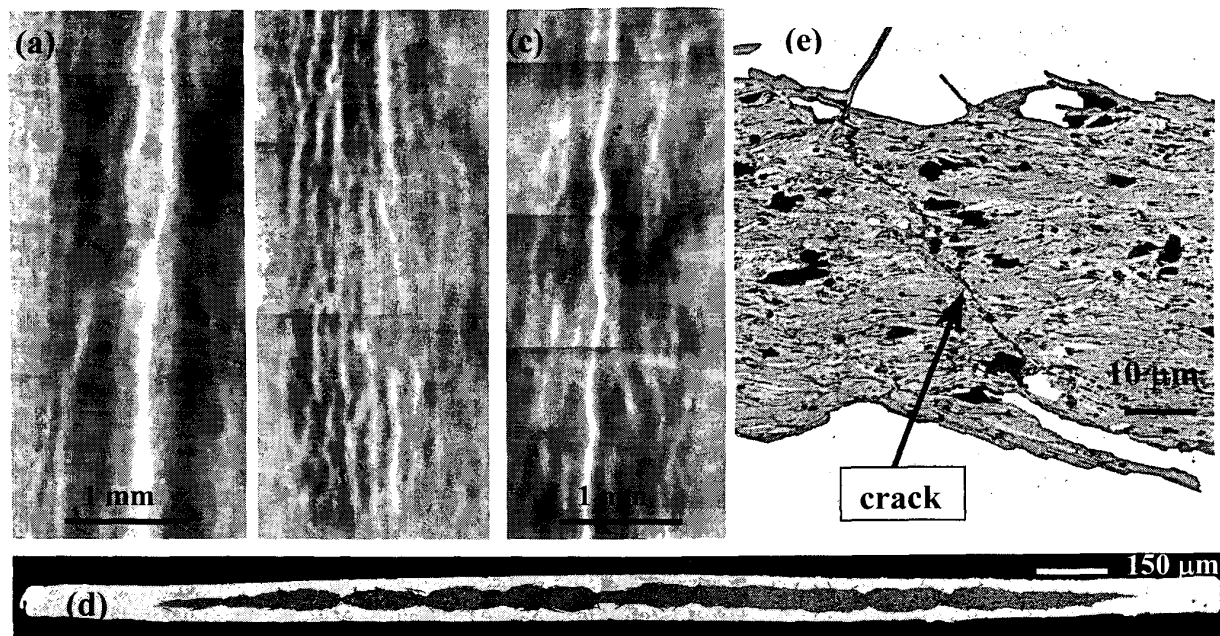


Fig. 5. a-c) Plan view magneto-optical (MO) images taken at 11K and 40 mT for tapes MO1-3, respectively. The dark regions shield magnetic flux very well while the light regions are of high magnetic flux density. d) Backscattered electron image of transverse cross section of tape MO2. e) Part of the image (d) with larger magnification, showing cracks.

Dark regions, especially in tape MO1 are well connected. As suggested by Han et al. [14], both rolling and pressing are inhomogeneous deformation processes. Although the critical current density was significantly improved after the fourth HT cycle shown in Fig. 4, the MO images indicate that cracks in the pressed tapes have not been fully healed during the final heat treatment, which is consistent with the SEM observation on the transverse cross section of tape MO2. Although the cracks in pressed tapes are less detrimental to the transport J_c than cracks formed in rolled tapes [7], it is clear from the MO images in Fig. 5 that the distribution of the cracks is not homogeneous and in particular some white lines are tortuous and form crack networks which are barriers to the current flow. This indicates that the performance of BSCCO-2223 tapes should be further improved by better controlling the deformation conditions and the liquid phase to better avoid and to heal the cracks.

IV. CONCLUSION

Higher J_c values ($\sim 35 \text{ kA/cm}^2$) have been achieved in mono-core Bi(Pb)-2223/Ag tapes made from the precursor powders with a lower formation rate of the Bi(Pb)-2223 phase. Reduction of Bi-2201 and nonsuperconducting phases is responsible for the higher J_c . However, longitudinal cracks caused by pressing have not been healed by heat treatment. This indicates that the performance of BSCCO-2223 tapes should be further improved by controlling the liquid phase to better heal the cracks.

ACKNOWLEDGEMENTS

The authors thank D. Apodaca, J. W. Anderson, X. Y. Cai, G. Yang, S. A. L. Foulds, D. Holdom and G. Bushnell-Wye for experimental help and discussion.

REFERENCES

- [1] S. X. Dou and H.K. Liu, *Supercond. Sci. Technol.*, vol. 6, 297, 1993
- [2] D. C. Larbalestier, X.Y. Cai, Y. Feng, H. Edelman, A. Umezawa, G. N. Riley Jr. and W.L. Carter, *Physica C*, vol. 221, 299, 1994
- [3] G. Grasso, A. Jeremie and R. Flükiger, *Supercond. Sci. Technol.* vol. 8, 827, 1995
- [4] X. Y. Cai, A. Polyanskii, Q. Li, G. N. Riley Jr., D. C. Larbalestier, *Nature*, vol. 392, 906, 1998
- [5] T. R. Thurston, U. Wildgruber, N. Jisrawi, P. Haldar, M. Suenaga, and Y.-L. Wang, *J. Appl. Phys.* Vol. 79, 3122, 1996
- [6] J. Jiang and J. S. Abell, *Physica C*, vol. 296, 13, 1998
- [7] J. P. Parrell, A. A. Polyanskii, A. E. Pashitski, and D. C. Larbalestier, *Supercond. Sci. Technol.*, vol. 9, 393, 1996
- [8] J. Jiang and J. S. Abell, *Supercond. Sci. Technol.*, vol. 11, 705, 1998
- [9] Y. E. High, Y. Feng, Y. S. Sung, E. E. Hellstrom, and D. C. Larbalestier, *Physica C*, vol. 220, 81, 1994
- [10] P. E. D. Morgan, R. M. Housley, J. R. Porter, and J. J. Ratto, *Physica C*, vol. 176, 279, 1991
- [11] Y.-L. Wang, W. Bain, Y. Zhu, Z.-X. Cai, D. O. Welch, R. L. Sabatini, M. Suenaga and T.R. Thurston, *Appl. Phys. Lett.*, vol. 69, 580, 1996
- [12] J.-C. Grivel, D. P. Grindatto, G. Grasso, and R. Flükiger, *Supercond. Sci. Technol.*, vol. 11, 110, 1998
- [13] W. G. Wang, J. Horvat, B. Zeimetz, H. K. Liu, and S. X. Dou, *Physica C*, vol. 291, 1, 1997
- [14] Z. Han P. Skov-Hensen and T. Freltoft, *Supercond. Sci. Technol.*, vol. 10, 371, 1997